Bulgarian Chemical Communications, Volume 50, Special Issue J (pp. 228–236) 2018

Sulfur and selenium derivatives of suberoyl anilide hydroxamic acid (SAHA) as a plausible HDAC inhibitors: a DFT study of their tautomerism and metal affinity/selectivity

D. Cheshmedzhieva*, N. Toshev, M. Gerova, O. Petrov, T. Dudev*

Faculty of Chemistry and Pharmacy, Sofia University "St. Kliment Ohridski", 1164 Sofia, Bulgaria

Received March, 2018; Revised May, 2018

Aberrations in histone deacetilase (HDAC) enzymes are associated with wide range of ailments including some types of cancer, inflammation, metabolic and neurological disorders. In a search for new efficient and body-tolerable HDAC inhibitors two analogs of hydroxamic acid drug (SAHA), containing sulfur- and selenium atoms in the carbonyl group of hydroxamic moiety have been investigated. Questions regarding their physico-chemical properties and metal affinity/selectivity have been addressed by employing density functional calculations combined with polarizable continuum model computations. More specifically, the paper answers the following questions: (1) How does the substitution in the hydroxamic group affect its conformational stability and ionization pattern? (2) What are the preferred deprotonation sites of the hydroxamic moiety and its mode of binding to the metal cation? (3) How does the O→S and O→Se exchange in hydroxamic moiety modulate its affinity and selectivity toward essential biogenic metal cations such as Mg^{2+}, Fe^{2+} and Zn^{2+}? The calculations reveal the key factors governing the ligation properties of the hydroxamic moiety and its sulfur and selenium analogs.

Keywords: Histone deacetylase inhibitors, SAHA, Sulphur derivatives, Selenium derivatives, DFT.

INTRODUCTION

There is an increasing evidence that epigenetic changes in gene expression play important role in progression of cancer. One of the important mechanisms of epigenetic regulation of gene expression is the acetylation and deacetilation of histones. This chromatin modification is controlled by two enzymes with opposing functions: histone acetyl transferases (HAT) and histone acetyl deacetylases (HDAC). The aberration in the action of these enzymes can alter the structure and function of chromatin and is associated with a wide range of ailments including some types of cancer [1, 2], inflammation [3], metabolic and neurological disorders [4, 5]. There are 18 HDACs grouped in four classes: Classes I, II and IV are metal (Zn^{2+} or Fe^{2+}) dependent hydrolases [6, 7]. Class III are NAD^+ dependent sirtuins and do not contain metal cation in the active site. Up to now several classes of small-molecule HDAC inhibitors (HDACi) have been recognized [8–11]. They reduce malignancies by blocking the cell cycle and inducing apoptosis [11] Most of these are hydroxamic acid derivatives, represented by suberoylanilide hydroxamic acid (SAHA) and trichostatin A (TSA) (Fig. 1). Their inhibitory effect stems from chelating the metal ion (Zn^{2+} or Fe^{2+}) in the active site of the enzyme and subsequent disruption of the host enzyme activity [8, 12]. Although hydroxamic acids are regarded as potent inhibitors, they generally have some issues associated with their use such as low oral availability, poor in vivo stability, and undesirable side effects [13, 14]. Therefore, the quest for more efficient and body-tolerable HDAC inhibitors is ongoing.

A series of sulfur and selenium-substituted derivatives of some HDAC inhibitors have been synthesized (Fig. 2) and probed for biological activity [15–17]. Thus, SAHA analogs containing α-mercaptoketone and α-thioacetoxyketone have been found to exhibit higher activity toward isolated histone deacetylases [15]. Derivatives of SAHA, containing one or two selenium atoms in different parts of the molecule (Fig. 2) were found to be 2 to 4-fold more selective against melanoma cells than the unmodified SAHA, and able to decrease melanoma tumor development by up to 87% with negligible toxicity [17, 18].

* To whom all correspondence should be sent:
E-mail: dvalentinova@gmail.com

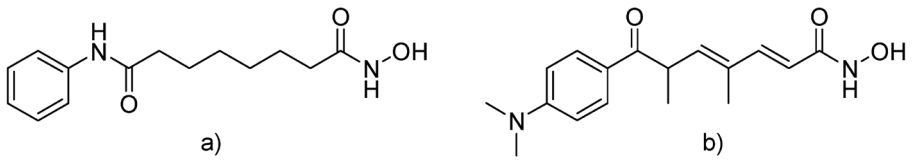

Fig. 1. Structure of a) suberoyl anilide hydroxamic acid (SAHA) and b) trichostatin A (TSA).

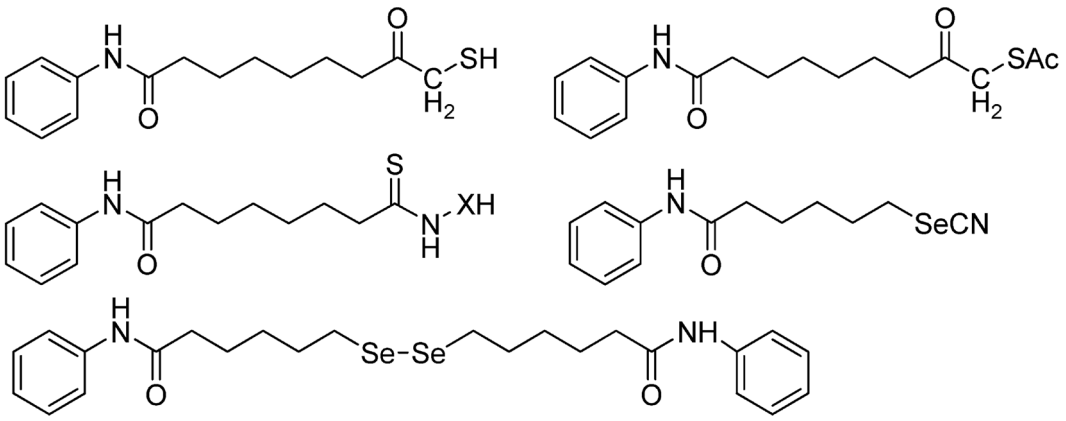

Fig. 2. Structure of sulfur and selenium analogs of SAHA.

Note that derivatives of SAHA where the hydroxamic ligating group –(C=O)−NHOH is modified to –(C=S)−NHOH and –(C=Se)−NHOH, have not been studied (to the best of our knowledge). To determine how incorporation of sulfur and selenium into the metal-binding part of SAHA changes its affinity/selectivity toward biogenic metal cations we modeled and examined the S- and Se-derivatives of the drug by combining density functional theory (DFT) calculations with polarizable continuum model (PCM) computations. In search for novel HDAC inhibitors we studied in detail the geometry and protonation pattern of sulfur- and selenium-containing analogs of SAHA. We investigated how the substitution of carbonyl oxygen in the hydroxamic group with sulfur (carb-S SAHA) and selenium (carb-Se SAHA) would affect its physicochemical and ligating properties as compared to the original unmodified molecule (carb-O SAHA). Several questions were addressed: (1) How does the substitution in the hydroxamic group affect its conformational stability and ionization pattern? (2) What are the preferred deprotonation sites of the hydroxamic moiety and its mode of binding to the metal cation? (3) How does the O→S and O→Se exchange in hydroxamic group modulate its affinity and selectivity toward essential biogenic metal cations such as Mg^{2+}, Fe^{2+} and Zn^{2+}? The calculations reveal the key factors governing the ligation properties of the hydroxamic moiety and its sulfur and selenium analogs.

COMPUTATIONAL METHODOLOGY

Sulfur and selenium carbonyl analogs of SAHA, called for convenience carb-S and carb-Se, were explicitly modeled. All the metal cations under study (Fe^{2+}, Mg^{2+} and Zn^{2+}) are usually hexahydrated in aqueous solution [19, 20]. Hence, their aqua complexes were modeled as $[M(H_2O)_6]^{2+}$ (M = Fe, Mg, Zn). In complexes with organic or protein ligands Mg^{2+} and Fe^{2+} usually retain the six-fold symmetry, whereas Zn^{2+} tend to reduce its coordination number to 4 and form complexes with tetrahedral symmetry [21–24]. Thus, complexes with octahedral symmetry between carb-X (X = O, S or Se) SAHA and Mg^{2+} and Fe^{2+} (high spin; quintuplet) were modeled, while for the complexes with Zn^{2+} tetrahedral symmetry was considered.

All calculations were performed with the Gaussian 09 suite of programs [25]. The B3LYP functional [26–28] in combination with 6-311++G(d,p) [29] basis set was employed in optimizing the structures of the molecules under study and evaluating the respective electronic energies, E_{el}^{ε}, in both the gas

phase (ε = 1) and solution. In the latter case polarizable continuum model (PCM) calculations in water (ε = 78) were performed. The combination between method and basis set was chosen based on: (i) previous theoretical studies on hydroxamic acids [30] and (ii) our own validation with respect to available experimental data [31].

Frequency calculations for each optimized structure were performed at the same level of theory. No imaginary frequency was found for the lowest energy configurations of any of the optimized structures. The vibrational frequencies were used to compute the thermal energies, E_{th}^{ε}, including zero-point energy, and entropies, S^{ε}.

The differences $\Delta E_{el}^{\varepsilon}$, $\Delta E_{th}^{\varepsilon}$, ΔPV (work term) and ΔS^{ε} between the products and reactants were used to evaluate the free energy of the product formation, ΔG^{ε}, in the gas phase and condensed media at T = 298.15 K according to:

$$\Delta G^{\varepsilon} = \Delta E_{el}^{\varepsilon} + \Delta E_{th}^{\varepsilon} + \Delta PV - T\Delta S^{\varepsilon} \qquad (1)$$

A positive ΔG^{ε} implies a thermodynamically unfavorable product formation, whereas negative value implies a favorable one. The free energy of deprotonation reaction in water solution (e = 78) were evaluated by employing the thermodynamic cycle shown in Scheme 1 where the experimental free energy of proton hydration (–264.0 kcal/mol [32]) was used.

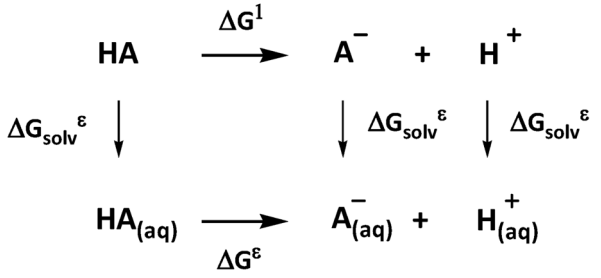

Scheme 1. Thermodynamic cycle employed for calculation of the free energy of deprotonation in solution.

$$\Delta G^{\varepsilon} = \Delta G^{1} + \Delta G_{solv}^{\varepsilon}\ (Products) - \Delta G_{solv}^{\varepsilon}\ (Reagents) \qquad (2)$$

RESULTS AND DISCUSSION

Tautomers of carb-S and carb-Se SAHA analogs. The main objective of this study is to assess how the substitution of oxygen atom from the hydroxamic carbonyl moiety by its analogs from the same group of the Periodic table, sulfur and selenium, could alter the tautomeric equilibria in carb-X SAHA. In answering this question, we modeled and thermodynamically characterized the respective S and Se derivatives of this molecule. Two possible tautomeric forms of hydroxamic acids could exist: keto and enol tautomers (Fig. 3). Furthermore, each tautomer can adopt *E*- or *Z*-conformation [33]. Four possible conformers for both S- and Se-derivatives have been modeled. The most stable form in the gas phase and in water solution is the 1Z-keto form (Table 1 and Fig. 3). The stabilization of 1Z tautomer is due to formation of intramolecular hydrogen bond between the -OH group and neighboring substituted carbonyl group (C=S, C=Se) as seen in

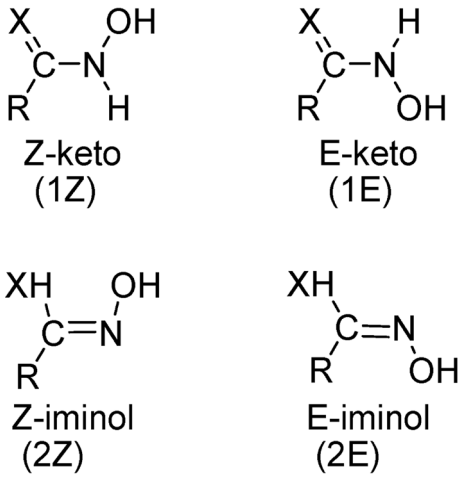

Fig. 3. Keto- and enol forms of hydroxamic acid derivatives; *E* and *Z* isomers.

Table 1. Relative Gibbs free energies (in kcal/mol) of the stable 1Z-keto and 1E-keto iminol tautomers of SAHA in the gas phase, ΔG_{SAHA}^{1}, and water, ΔG_{SAHA}^{78}

	$\Delta G_{carb\text{-}O\text{-}SAHA}^{1}$	$\Delta G_{carb\text{-}S\text{-}SAHA}^{1}$	$\Delta G_{carb\text{-}Se\text{-}SAHA}^{1}$	$\Delta G_{carb\text{-}O\text{-}SAHA}^{78}$	$\Delta G_{carb\text{-}S\text{-}SAHA}^{78}$	$\Delta G_{carb\text{-}Se\text{-}SAHA}^{78}$
1Z	0.0	0.0	0.0	0.0	0.0	0.0
1E	2.1	5.0	5.4	1.9	5.0	4.2
2Z	2.7	0.6	1.1	5.4	3.2	3.8

Fig. 4. The calculations reveal that in all the analogs of SAHA the most stable conformer is the 1Z-keto form (Table 2), as in the unmodified molecule (Table 2). As compared to the unmodified carb-O SAHA molecule, the free energy difference between the 1Z-keto and 1E-keto forms in the heavier-element derivatives are more pronounced (Table 1). Interestingly, the 2Z iminol form in carb-S SAHA (Fig. 4C) carb-Se SAHA appear quite close in energy (just 0.6 kcal/mol and 1.1 kcal/mol free energy difference respectively) to the 1Z conformer due to the stabilization effect of the intramolecular hydrogen bond. The two most stable conformers for the substituted SAHA analogs are 1Z and 2Z and here is the big difference in comparison to the parent compound carb-O SAHA, where the two most stable conformers are 1Z and 1E (both keto forms).

Hydroxamic acids are weak acids with two labile acidic protons in the hydroxamic moiety (–OH and –NH (Fig. 1)) which could be detached in the

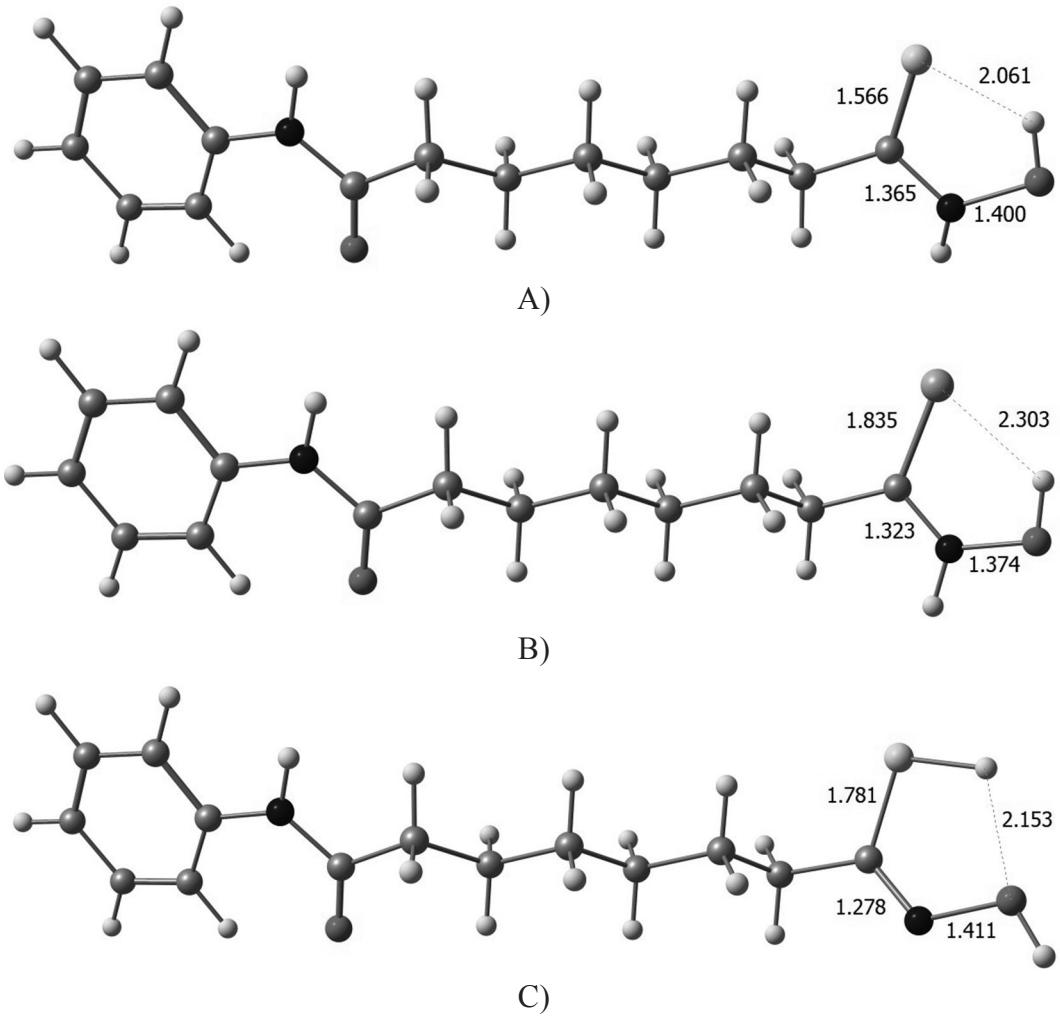

Fig. 4. The optimized geometries of A) 1Z-keto form of carb-S SAHA, B) 1Z-keto form of carb-Se SAHA C) carb-S SAHA 2Z conformer at B3LYP/6-311++G(d,p) level of theory.

Table 2. Change in the Gibbs free energies (in kcal/mol) in the gas phase and water for the reaction of deprotonation of SAHA ($AH \rightarrow A^- + H^+$). $\Delta G_{solv}^{78}(H^+)$ of –264.0 kcal/mol is taken from the experiment [32]

	$\Delta G_{carb\text{-}O\text{-}SAHA}^{1}$	$\Delta G_{carb\text{-}S\text{-}SAHA}^{1}$	$\Delta G_{carb\text{-}Se\text{-}SAHA}^{1}$	$\Delta G_{carb\text{-}O\text{-}SAHA}^{1}$	$\Delta G_{carb\text{-}S\text{-}SAHA}^{78}$	$\Delta G_{carb\text{-}Se\text{-}SAHA}^{78}$
1Z deprotonated O	347.9	336.7	333.4	24.6	17.5	15.8
1Z deprotonated N	334.2	319.6	316.3	19.9	9.6	7.9

course of chemical/biochemical reaction thus bestowing an OH- or NH-acid properties, respectively, on the parent molecules. [39] What is the deprotonation pattern of the S- and Se-analogs of SAHA? In order to shed light on this question, we modeled the two deprotonation pathways in carb –S/Se SAHA analogs (through OH or NH deprotonation) and evaluated their thermodynamic efficiency (Table 2). The calculations demonstrate that the most stable deprotonated form in the carb –S SAHA derivative in the gas phase is the N-deprotonated 1Z form (Fig. 5b), which is 17.1 kcal/mol more stable in the gas-phase and 7.9 kcal/mol in water medium than the O-deprotonated 1Z form (Table 2). For the Se derivative, these numbers are exactly the same. The stabilization of the N-deprotonated 1Z form is mainly due to the intramolecular hydrogen bond, which is preserved from the original parent structure (structure not shown). The calculations (Table 2) show that carbonyl S- and Se- analogs of SAHA, like the parent unmodified carbonyl O-construct [34] behave essentially as NH acids in both the gas phase and water solution. Data collected in Table 2 reveal that the heavier the heteroatom in the C=O/C=S/C=Se group, the more favorable the proton dissociation at NH location is (decreased free energies of deprotonation in the sequence C=O > C=S > C=Se).

Metal selectivity of SAHA. The nature of the metal cofactor at the enzyme active center greatly affects the thermodynamics and kinetics of the interactions with the respective substrates and enzyme inhibitors. In proteins very often metal cations such as Mg^{2+}, Zn^{2+} and Fe^{2+} compete for the same binding site [20, 35–38] and the proper metal cofactor is selected either by the protein itself or by the cell machinery which strictly regulates the free metal concentration in the intracellular compartments [439]. Note that the identity of the native metal cofactor at the active site of HDACs is still not resolved. Transition metal dications, such as Zn^{2+}, Co^{2+} and Fe^{2+} have been implicated in the enzyme activation. Note, that examples exist of metal-dependent enzymes (including HDAC) that have been reclassified from Zn^{2+}-dependent to Fe^{2+}-dependent enzymes [40–43]. Thus, it is of particular interest to study the metal binding properties of the carb-X (X = O, S, Se) SAHA analogs as possible HDAC inhibitors towards different biogenic metal cations and elucidate the major factors controlling their metal affinity and selectivity.

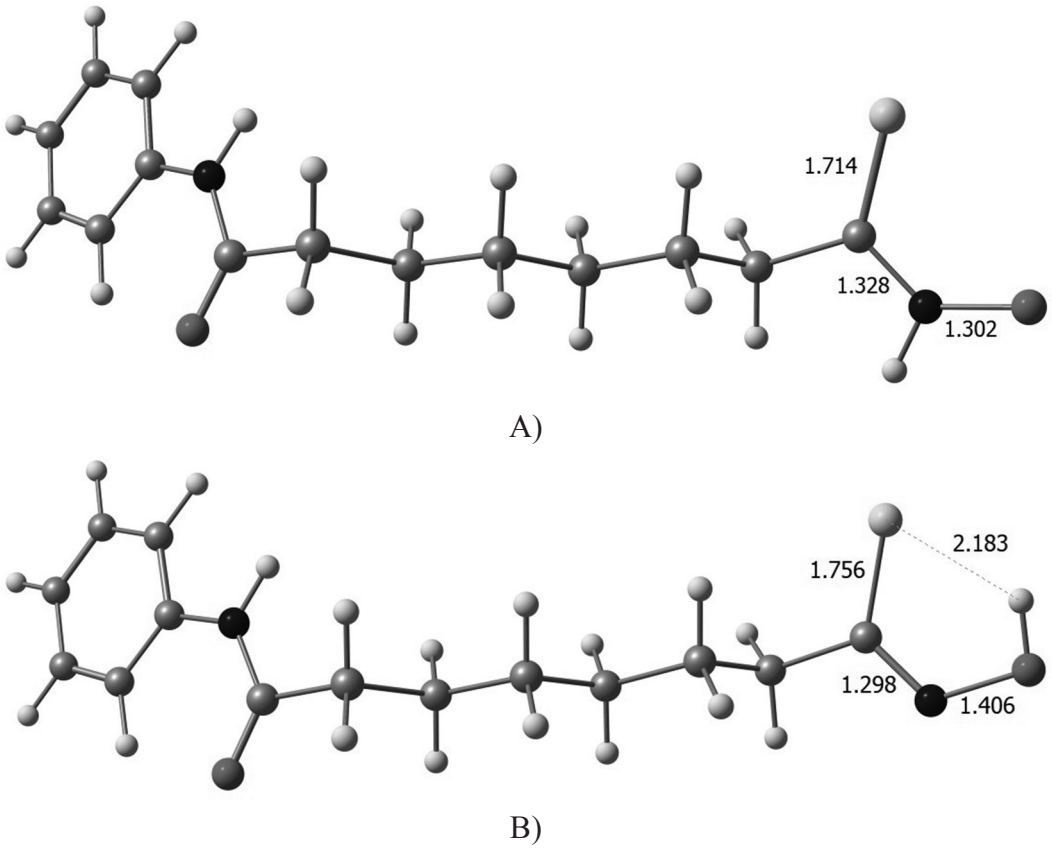

Fig. 5. B3LYP/6-311++G(d,p) optimized structures of carb-S SAHA deprotonated at (A) OH and (B) NH site of the hydroxamic moiety. Bond lengths are given in Å.

Table 3. Change in the Gibbs free energy (in kcal/mol, ΔG^1 gas phase, ΔG^{78} in water) for the $Mg^{2+} \rightarrow Zn^{2+}$exchange reactions in SAHA, carb-S SAHA, carb-Se SAHA complexes

	ΔG^1	ΔG^{78}
$[Mg(H_2O)_6]^{2+} + [SAHA\text{-}Zn(H_2O)_2]^+ + 2H_2O \rightarrow [Zn(H_2O)_6]^{2+} + [SAHA\text{-}Mg(H_2O)_4]^+$	–1.7	20.7
$[Mg(H_2O)_6]^{2+} + [carb\text{-}S\ SAHA\text{-}Zn(H_2O)_2]^+ + 2H_2O \rightarrow [Zn(H_2O)_6]^{2+} + [carb\text{-}S\ SAHA\text{-}Mg(H_2O)_4]^+$	9.4	31.5
$[Mg(H_2O)_6]^{2+} + [carb\text{-}Se\ SAHA\text{-}Zn(H_2O)_2]^+ + 2H_2O \rightarrow [Zn(H_2O)_6]^{2+} + [carb\text{-}Se\ SAHA\text{-}Mg(H_2O)_4]^+$	2.9	30.9

ΔG^1 the free energy change for the reaction in gas phase, ΔG^{78} – in water.

Table 4. Change in the Gibbs free energy (in kcal/mol) for the $Fe^{2+} \rightarrow Zn^{2+}$exchange reactions in SAHA, SAHA-S, SAHA-Se complexes

	ΔG^1	ΔG^{78}
$[Fe(H_2O)_6]^{2+} + [SAHA\text{-}Zn(H_2O)_2]^+ + 2H_2O \rightarrow [Zn(H_2O)_6]^{2+} + [SAHA\text{-}Fe(H_2O)_4]^+$	–6.4	16.4
$[Fe(H_2O)_6]^{2+} + [carb\text{-}S\ SAHA\text{-}Zn(H_2O)_2]^+ + 2H_2O \rightarrow [Zn(H_2O)_6]^{2+} + [carb\text{-}S\ SAHA\text{-}Fe(H_2O)_4]^+$	0.1	19.2
$[Fe(H_2O)_6]^{2+} + [carb\text{-}Se\ SAHA\text{-}Zn(H_2O)_2]^+ + 2H_2O \rightarrow [Zn(H_2O)_6]^{2+} + [carb\text{-}Se\ SAHA\text{-}Fe(H_2O)_4]^+$	2.9	19.3

ΔG^1 the free energy change for the reaction in gas phase, ΔG^{78} – in water.

The SAHA metal ion selectivity can be expressed in terms of the free energy, ΔG^{ε}, for replacing Zn^{2+} bound to the inhibitor by its rival cation, M^{2+} (M = Mg, Fe):

$$[Mg(H_2O)_6]^{2+} + [carb\text{-}X\ SAHA\text{-}Zn(H_2O)_2]^+ + 2H_2O \rightarrow [Zn(H_2O)_6]^{2+} + [carb\text{-}X\ SAHA\text{-}Mg(H_2O)_4]^+ \quad (4)$$

$$[Fe(H_2O)_6]^{2+} + [carb\text{-}X\ SAHA\text{-}Zn(H_2O)_2]^+ + 2H_2O \rightarrow [Zn(H_2O)_6]^{2+} + [carb\text{-}X\ SAHA\text{-}Fe(H_2O)_4]^+ \quad (5)$$

In this model the carb-S and carb-Se derivatives are in their O-deprotonated form and the total charge of the metal complexes is +1. In a previous study [31] it was shown that even SAHA shows NH acidity in gas phase and solution the preferred form of complexation is with O-deprotonated form. In eqs. 4 and 5 a positive ΔG^{ε} implies a Zn^{2+}-selective ligand whereas a negative value implies a Mg^{2+}/Fe^{2+} selective one. The thermodynamic parameters evaluated for carb-X SAHA in the gas phase and condensed media are summarized in Tables 3 and 4. Optimized structures of the metal complexes are shown in Fig. 6. Calculations imply that in the gas phase the substitution reactions for the unmodified SAHA are favorable (negative ΔG^1) but become unfavorable for the S- and Se-substituted analogs evidenced by positive free energies of $Zn^{2+} \rightarrow Mg^{2+}$ and $Zn^{2+} \rightarrow Fe^{2+}$ exchange. This implies that it will be difficult for both metal cations to replace Zn^{2+} in these complexes. The S- and Se-containing SAHA derivatives exhibit higher Zn^{2+} selectivity in condensed media relative to SAHA as well (higher free energies of metal exchange in Tables 3 and 4). The "softer" character of the Zn^{2+} cation relative to that of the Fe^{2+} and Mg^{2+} cations favors the interactions between Zn^{2+} and the "soft" S- and Se-containing ligands in greater extent than those between Fe^{2+} and Mg^{2+} and carb-S SAHA/carb-Se SAHA.

CONCLUSIONS

A systematic theoretical study on sulfur and selenium derivatives of a representative of the family of the HDAC inhibitors – SAHA, has been performed using density functional theory combined with polarizable continuum model calculations. The relative stability of different conformers of the studied molecules was determined. In all cases the most stable is 1Z keto form. The energies of depro-

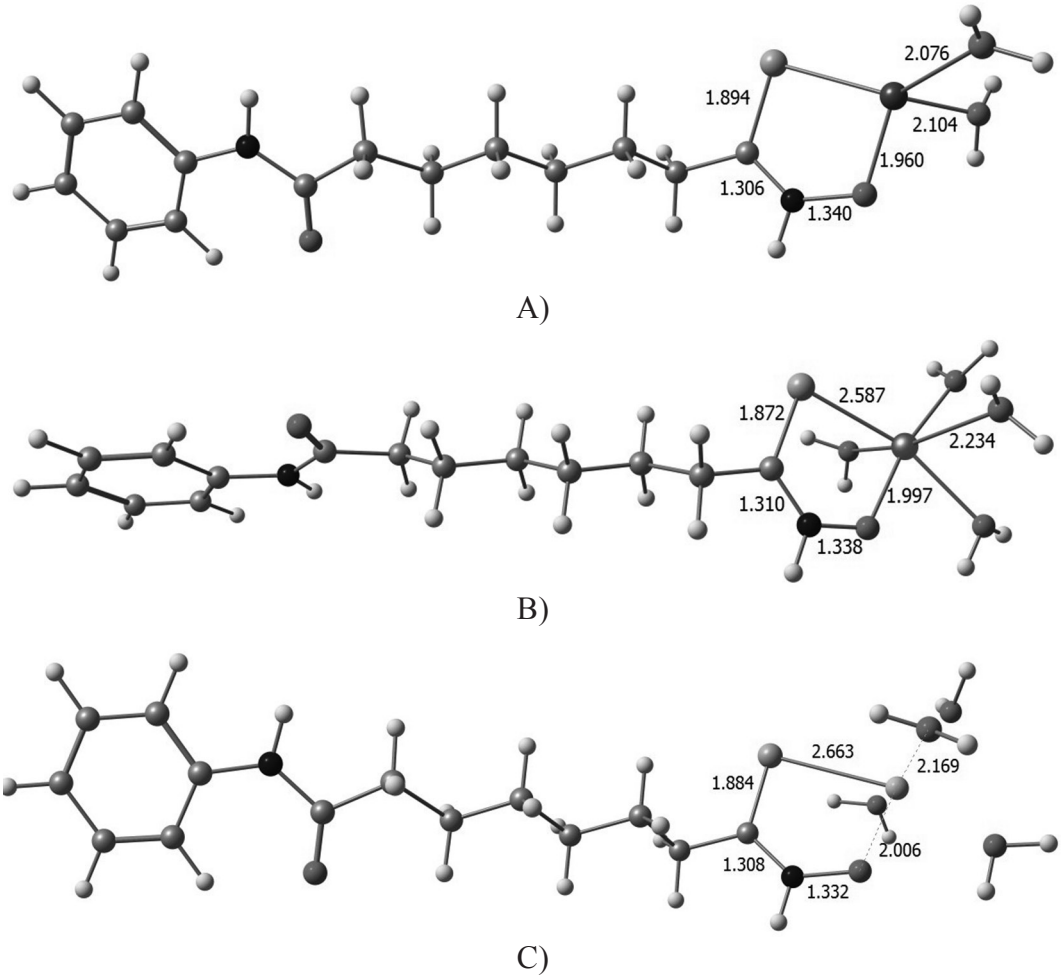

Fig. 6. Optimized structures at B3LYP/6-311++G(d,p) level of theory for the complexes of carb-Se SAHA with A) Zn^{2+}, B) Fe^{2+} and C) Mg^{2+}.

tonation for the two possible ionizable groups, O-H and N-H, are also determined. It has been found that for the metal-free molecule thermodynamically more favorable is the deprotonation of the N-H group. Sulfur and selenium-containing analogs are deprotonated more easily than the parent SAHA molecule. Deprotonation at the N-H site is more favorable for both compounds. In condensed media SAHA and its sulfur and selenium analogs exhibit greater affinity/selectivity toward Zn^{2+} cations with a noticeable increase in the order O < S ~ Se.

REFERENCES

1. (a) T. Kouzarides, *Curr. Opin. Genet. Dev.*, **9**, 40 (1999). (b) A. H. Lund., M. von Lohuizen, *Genes Dev*., **18** (19), 2315 (2004). (c) S. B. Baylin, J. E. Ohm, *Nature Rev. Cancer*, **6**, 107 (2006).
2. R. Fendrick, S. W. Hiebert, *J. Cell. Biochem. (Suppl.)*, **30–31**, 194 (1998).
3. M. R. Shakespear, M. A. Halili, K. M. Irvine, D. P. Fairlie, M. J. Sweet, *Trends Immunol*., **323**, 35 (2011).
4. J. Gräff, D. Kim, M. M. Dobbin, L. H. Tsai, *Physiol. Rev.*, **91**, 603 (2011).
5. N. L. Wiech, J. F. Fisher, P. Helquist, O. Wiest, *Curr. Top Med. Chem.*, **9**, 257 (2009).
6. D. P. Dowling, S. L. Gantt, S. G. Gattis, C. A. Fierke, D. W. Christianson, *Biochemistry*, **47**, 13554 (2008).
7. (a) S. L. Gantt, S. G. Gattis, C. A. Fierke, *Biochemistry*, **45**, 6170 (2006). (b) S. L. Gantt, C. G. Joseph, C. A. Fierke, *J. Biol. Chem*., **285**, 6036 (2010).
8. J. R. Somoza, R. J. Skene, B. A. Katz, C. Mol, J. D. Ho, A. J. Jennings, C. Luong, A. Arvai, J. J. Buggy, E. Chi, J. Tang, B. C. Sang, E. Verner, R. Wynands, E. M. Leahy, D. R. Dougan, G Snell, M. Navre, M. W. Knuth, R. V. Swanson, D. E. McRee, L. W. Tari, *Structure*, **12**, 1325 (2004).
9. M. Mottamal, S. Zheng, T. L. Huang, G. Wang, *Molecules*, **20**, 3898 (2015).
10. T. A. Miller, D. J. Witter, S. J. Belvedere, *Med. Chem.*, **46**, 5097 (2003).

11. O. Khan, N. B. La Thangue. *Immunol Cell. Biol.*, **90**, 85 (2012).
12. M. S. Finnin, J. R. Donigian, A. Cohen, V. M. Richon, R. A. Rifkind, P. A. Marks, R. Breslow, N. P. Pavletich, *Nature*, **401**, 188 (1999).
13. S. Vassiliou, A. Mucha, P. Cuniasse, D. Georgiadis, K. Lucet-Levannier, F. Beau, R. Kannan, G. Murphy, V. Knaeuper, C. M. Rio, P. Basset, A. Yiotakis, V. Dive. *J. Med Chem.*, **42**, 2610 (1999).
14. G. J. Mulder, J. H. Meerman, *Environ. Health Perspect.*, **49**, 27 (1983).
15. T. Suzuki, A. Kouketsu, A. Matsuura, A. Kohara, S. Ninomiya, K. Kohda, N. Miyata, *Bioorg Med Chem Lett.*, **14**, 3313 (2004).
16. W. Gu, I. Nusinzon, R. D. Smith Jr, C. M. Horvath, R. B. Silverman, *Bioorg. Med. Chem.*, **14**, 3320 (2006).
17. D. Desai, U. Salli, K. E. Vrana, S. Amin, *Bioorg. Med. Chem. Lett*., **20**, 2044 (2010).
18. R. Gowda, S. V. Madhunapantula, D. Desai, S. Amin, G. P. Robertson, *Cancer Biol. Ther*., **13**, 756 (2012).
19. Y. Marcus, *Chem. Rev.*, **88**, 1475 (1988).
20. M. Dudev, J. Wang, T. Dudev, C. Lim, *J. Phys. Chem. B*, **110**, 1889 (2006).
21. T. Dudev, C. Lim, *J. Am. Chem. Soc.*, **122**, 11146 (2000).
22. T. Dudev, C. Lim, *J. Phys. Chem. B*, **105**, 4446 (2001).
23. J. M. Berg, H. A. Godwin, *Annu. Rev. Biophys. Biomol. Struct.*, **26**, 357 (1997).
24. W. Gong, X. Zhu, S. Liu, M. Teng, L. Niu, *J. Mol. Biol.*, **283**, 657 (1998).
25. M. J. Frisch, G. W. Trucks, H. B. Schlegel, G. E. Scuseria, M. A. Robb, J. R. Cheeseman, G. Scalmani, V. Barone, G. A. Petersson, H. Nakatsuji, X. Li, M. Caricato, A. Marenich, J. Bloino, B. G. Janesko, R. Gomperts, B. Mennucci, H. P. Hratchian, J. V. Ortiz, A. F. Izmaylov, J. L. Sonnenberg, D. Williams-Young, F. Ding, F. Lipparini, F. Egidi, J. Goings, B. Peng, A. Petrone, T. Henderson, D. Ranasinghe, V. G. Zakrzewski, J. Gao, N. Rega, G. Zheng, W. Liang, M. Hada, M. Ehara, K. Toyota, R. Fukuda, J. Hasegawa, M. Ishida, T. Nakajima, Y. Honda, O. Kitao, H. Nakai, T. Vreven, K. Throssell, J. A. Montgomery, Jr., J. E. Peralta, F. Ogliaro, M. Bearpark, J. J. Heyd, E. Brothers, K. N. Kudin, V. N. Staroverov, T. Keith, R. Kobayashi, J. Normand, K. Raghavachari, A. Rendell, J. C. Burant, S. S. Iyengar, J. Tomasi, M. Cossi, J. M. Millam, M. Klene, C. Adamo, R. Cammi, J. W. Ochterski, R. L. Martin, K. Morokuma, O. Farkas, J. B. Foresman, D. J. Fox, Gaussian09, Revision A.02, Gaussian, Inc., Wallingford CT, 2009.
26. A. D. Becke, *J. Chem. Phys.*, **98**, 5648 (1993).
27. A. D. Becke, *J. Chem. Phys.*, **104**, 1040 (1996).
28. C. T. Lee, W. T. Yang, R. G. Parr, *Phys. Rev. B*, **37**, 785(1988).
29. K. Raghavachari, J. S. Binkley, R. Seeger, J. A. Pople, *J. Chem. Phys*., **72**, 650 (1980).
30. R. Kakkar, R. Grover, P. Chadha, *Org. Biomol. Chem.*, **1**, 2200 (2003).
31. D. Cheshmedzhieva, N. Toshev, M. Gerova, O. Petrov, T. Dudev, *J. Mol. Model.*, **24**, 114 (2018).
32. M. D. Tissandier, K. A. Cowen, W. Y. Feng, E. Gundlach, M. H. Cohen, A. D. Earhart, J. V. Coe, T. R. Tuttle Jr., *J. Phys. Chem. A*, **102**, 7787 (1998).
33. D. Brown, W. Glass, B. G. R. Mageswaren, *Mag. Res. Chem.*, **26**, 1705 (1988).
34. M. Decouzon, O. Exner, J. F. Gal, P. C. Maria, *J. Org. Chem.*, **55**, 3980 (1990).
35. P. Ciancaglini, J. M. Pizauro, C. Curti, A. C. Tedesco, F. A. Leone, *Int. J. Biochem*., **22**, 747 (1990).
36. G. S. Lukat, A. M. Stock, J. B. Stock, *Biochemistry*, **29**, 5436 (1990).
37. G. Sun, R. J. A. Budde, *Biochemistry*, **38**, 5659 (1999).
38. L. V. Lee, R. R. Poyner, M. V. Vu, W. W. Cleland, *Biochemistry*, **39**, 4821 (2000).
39. T. Dudev, C. Lim, *Chem. Rev*., **114**, 538 (2014).
40. B. C. Tripp, C. B. Bell III, F. Cruz, C. Krebs, J. G. Ferry, *J. Biol. Chem*., **279**, 6683 (2004).
41. J. Zhu, E. Dizin, X. Hu, A. S. Wavreille, J. Park, D. Pei. *Biochemistry*, **42**, 4717 (2003).
42. D. P. Dowling, S. G. Gattis, C. A. Fierke, D. W. Christianson, *Biochemistry*, **49**, 5048 (2010).
43. B. Kim, A. S. Pithadia, C. A. Fierke, *Protein Sci*., **24**, 354 (2015).

СЯРА И СЕЛЕН СЪДЪРЖАЩИ ПРОИЗВОДНИ НА СУБЕРОИЛ АНИЛИД ХИДРОКСАМОВА КИСЕЛИНА (SAHA) КАТО ПОТЕНЦИАЛНИ HDAC ИНХИБИТОРИ: DFT ИЗСЛЕДВАНЕ НА ТАВТОМЕРИЯТА И МЕТАЛНИЯ ИМ АФИНИТЕТ/СЕЛЕКТИВНОСТ

Д. Чешмеджиева*, Н. Тошев, М. Герова, О. Петров, Т. Дудев*

Факултет по химия и фармация, Софийски университет „Св. Климент Охридски“, бул. Дж. Баучер 1, 1164 София, България

Постъпила март, 2018 г.; приета май, 2018 г.

(Резюме)

Нарушаването на действието на ензимите от групата на хистон деацетилазите (HDAC) се свързва с широк спектър от заболявания, включително някои видове рак, възпаления, метаболитни и неврологични заболявания. В търсене на нови ефикасни и по-толерантни HDAC инхибитори, са изследвани два аналога на утвърденото лекарство субероил анилид хидроксамова киселина (SAHA), съдържащи серни и селенови атоми в карбонилната група на хидроксамовия остатък. С помощта на теорията на плътностния функционал (density functional theory – DFT) са изследвани техните физикохимични свойства както и афинитета/селективността им към метали в газова фаза и разтворител. По-конкретно, статията отговаря на следните въпроси: (1) Как заместването в хидроксамовата група влияе върху нейната конформационна стабилност? (2) Какви са предпочитаните места за депротониране на хидроксамовата част и начина на свързване към металния катион? (3) Как обменът на O → S и O → Se в хидроксамовата част модулира афинитета и селективността към основни биогенни метални катиони като Mg^{2+}, Fe^{2+} и Zn^{2+}? Изчисленията разкриват ключовите фактори, определящи лигиращите свойства на хидроксамовата част на инхибитора и нейните серни и селенови аналози.